Experimental Eye Research 166 (2018) 160–167

Contents lists available at ScienceDirect

Experimental Eye Research

journal homepage: www.elsevier.com/locate/yexer

Furin deficiency in myeloid cells leads to attenuated revascularization in a mouse-model of oxygen-induced retinopathy

Maria Vähätupa[a], Zuzet Martinez Cordova[a,b], Harlan Barker[a], Saara Aittomäki[a,b], Hannu Uusitalo[a,c,*], Tero A.H. Järvinen[a,d], Marko Pesu[a,b,e], Hannele Uusitalo-Järvinen[a,c]

[a] Faculty of Medicine & Life Sciences, University of Tampere, Tampere, Finland
[b] Immunoregulation, Institute of Biosciences and Medical Technology (BioMediTech), University of Tampere, Tampere, Finland
[c] Eye Centre, Tampere University Hospital, Tampere, Finland
[d] Departments of Musculoskeletal Disorders, Tampere University Hospital, Tampere, Finland
[e] Departments of Dermatology, Tampere University Hospital, Tampere, Finland

ARTICLE INFO

Keywords:
Angiogenesis
Furin
Macrophage
Oxygen-induced retinopathy model
Hypoxia

ABSTRACT

Ischemic retinopathy is a vision-threatening disease associated with chronic retinal inflammation and hypoxia leading to abnormal angiogenesis. Furin, a member of the proprotein convertase family of proteins, has been implicated in the regulation of angiogenesis due to its essential role in the activation of several angiogenic growth factors, including vascular endothelial growth factor-C (VEGF-C), VEGF-D and transforming growth factor - β (TGF- β). In the present study, we evaluated expression of furin in the retina and its role in retinal angiogenesis. As both inflammation and hypoxia contribute to angiogenesis, the role of furin was evaluated using myeloid-cell specific furin knockout (KO) mice (designated LysMCre-fur$^{(fl/fl)}$) both in developmental retinal angiogenesis as well as in hypoxia-driven angiogenesis using the oxygen-induced retinopathy (OIR) model. In the retina, furin expression was detected in endothelial cells, macrophages and, to some extent, in neurons. The rate of angiogenesis was not different in LysMCre-fur$^{(fl/fl)}$ mice when compared to their wild-type littermates during development. In the OIR model, the revascularization of retina was significantly delayed in LysMCre-fur$^{(fl/fl)}$ mice compared to their wild-type littermates, while there was no compensatory increase in the preretinal neovascularization in LysMCre-fur$^{(fl/fl)}$ mice. These results demonstrate that furin expression in myeloid cells plays a significant role in hypoxia-induced angiogenesis in retina.

1. Introduction

Ischemic retinopathies, such as retinopathy of prematurity (ROP), proliferative diabetic retinopathy (PDR), and retinal vein occlusion (RVO) are major causes of visual impairment and blindness in industrialized countries (Fong et al., 2004; Jonas et al., 2017; Reynolds, 2014). Retinal ischemia induces the stabilization of a transcription factor hypoxia inducible factor-1α (HIF-1α), which turns on the expression of a large number of angiogenic genes such as vascular endothelial growth factor (VEGF) (Campochiaro, 2015). This leads to retinal neovascularization associated with vitreous hemorrhages and fibrosis of neovascular membranes causing tractional retinal detachment and, ultimately, blindness (Campochiaro, 2015).

Retinal ischemia is also associated with inflammatory manifestations. Hypoxia attracts macrophages into hypoxic areas (Mitamura et al., 2005; Tsutsumi et al., 2003) where the hypoxia-activated macrophages and microglia, the immune cells of the retina, release not only proinflammatory but also angiogenic cytokines. In diabetic retinopathy (DR), both invading macrophages and resident microglia have been implicated in the pathogenesis of the retinopathy retinopathy (Abcouwer, 2012). Of note, macrophages have been shown to be the main source of VEGF-C in the retina. In the retina, VEGF-C signaling pathway regulates the branching of blood vessels (Tammela et al., 2011). VEGF-C is initially synthesized as an inactive precursor and requires activation by a proprotein convertase subtilisin/kexin (PCSK) family member furin to become biologically active (Siegfried et al., 2003b).

Proprotein convertase subtilisin/kexin (PCSK) family enzymes are a family of nine proteases (PCSK1-2, furin, PCSK4-7, MBTPS1, PCSK9) that cleave and convert their immature target proteins into biologically active forms by catalyzing endoproteolytic cleavage at a target site typically made up of the basic amino acids arginine and lysine (Turpeinen et al., 2013). Accordingly, PCSK enzymes play a key regulatory role in a multitude of biological events governed by the growth

* Corresponding authorFaculty of Medicine & Life Sciences, 33014, University of Tampere, Finland.
E-mail address: llhauus@uta.fi (H. Uusitalo).

https://doi.org/10.1016/j.exer.2017.10.013
Received 4 January 2017; Received in revised form 1 September 2017; Accepted 11 October 2017
Available online 13 October 2017

factors (Turpeinen et al., 2013). Among the PCSK family members, furin is a ubiquitously expressed prototypical serine endoprotease recently implicated to play a key role in various biological processes such autoimmunity and inflammation, and various human diseases (Oksanen et al., 2014; Pesu et al., 2008; Turpeinen et al., 2013; Vähätupa et al., 2016a). In fibrovascular tissue from PDR patients, furin expression was shown to co-localize with one of its cleavage targets, a (pro)-renin receptor protein, whose expression level is elevated in PDR and associated with angiogenic activity, suggesting that furin cleavage has a role in DR (Kanda et al., 2012).

In addition to VEGF-C (Khatib et al., 2010; Siegfried et al., 2003a), furin is also required for the activation of a large number of other proangiogenic growth factors, such as VEGF-D (McColl et al., 2007), platelet derived growth factors A and B (PDGF-A and –B) (Siegfried et al., 2003b, 2005), bone morphogenetic protein-4 (BMP-4) (Cui et al., 1998) and transforming growth factor-β (TGF-β) (Dubois et al., 2001). On the other hand, the expression of furin itself can be induced by hypoxia, as it is one of the target genes of HIF-1α (Ma et al., 2017; McMahon et al., 2005; Silvestri et al., 2008). Despite being linked to angiogenesis, the functions of furin in these processes are still poorly known, but the phenotype of the total furin knockout (KO) mice, lethality during embryonal development due to cardiovascular defects, suggested blood vessel specific functions (Roebroek et al., 1998; Scamuffa et al., 2006). This notion was confirmed by endothelial specific furin KO that also led to embryonal death due to vascular defects, and by the endothelial cells lacking furin that were unable to grow *ex vivo* (Kim et al., 2012).

As endothelial cells lacking furin cannot grow at all (Kim et al., 2012), we decided to elucidate the role of furin on retinal angiogenesis by addressing the expression of furin in the retina and by assessing the effect of myeloid cell-derived furin on retinal angiogenesis using furin conditional KO mice (myeloid cell-specific furin KO; LysMCre-fur$^{(fl/fl)}$). The effect of myeloid cells-derived furin on angiogenesis was studied in developmental retinal angiogenesis, as well as in hypoxia-induced angiogenesis in a mouse-model for oxygen-induced retinopathy (OIR), which is the most widely used model for ischemic retinopathies (Connor et al., 2009; Smith et al., 1994). In the OIR model, both recruited, blood-derived macrophages as well as the resident macrophages of the retina, microglia, have been shown to participate in the regulation of angiogenesis (Checchin et al., 2006; Gao et al., 2016; Kataoka et al., 2011; Zhou et al., 2015).

2. Results

2.1. Furin is expressed in macrophages and retinal microglia

Using data from published genome-wide expression studies, the retinal-cell specific E-GEOD-33089 experiment and the much wider searching FANTOM project, we extracted expression data for furin in cells related to retina. In the larger, but far less specific, FANTOM project cDNA analysis of furin expression showed the highest values in monocyte derived macrophages (Fig. 1A). In the retinal cell-specific experiment, based on 155 samples analyzed by microarray, the highest furin expression was found in microglia (Fig. 1B).

2.2. Furin is expressed in the retina during development and in the OIR model

To further study the role of furin on retinal angiogenesis *in vivo*, we first determined a temporal and spatial expression profile of furin in WT mice during development and in the OIR model. Immunohistochemistry showed a few cells with weak expression of furin in retina at P4 (postnatal day 4), and thereafter the expression of furin was substantially stronger from P7 onwards at all studied time points during development (Fig. 1C). In the OIR model, strong expression of furin was detected in the vascular layers of the retina at P14 and P17 (Fig. 1D). Using double-immunohistochemistry for furin and for endothelial cells marker CD31 as well as for furin and macrophage marker F4/80, furin expression was localized to endothelial cells (Fig. 1E–F) in the retina and in the preretinal vascular tufts as well as to macrophages surrounding blood vessels (Fig. 1G–H) in OIR retinas. In addition to these cells, furin immunoreactivity was also detected in neurons in the retina (Fig. 1).

2.3. Lack of furin in myeloid cells does not influence the rate of developmental angiogenesis

To investigate the role of furin in angiogenesis, we studied mice deficient for *furin* gene expression in myeloid cells (LysMCre-fur$^{(fl/fl)}$) and their respective wild-type littermates (LysM WT) during developmental retinal angiogenesis and during ischemia induced retinal angiogenesis using oxygen-induced retinopathy model (OIR). LysMCre-fur$^{(fl/fl)}$ mice are fertile without no obvious morphological abnormalities (Cordova et al., 2016), and their eyes appear normal upon histological examination. As total depletion of resident retinal macrophages has been shown to slow down the rate of developmental retinal angiogenesis (Checchin et al., 2006), we first explored whether myeloid cell derived furin influences the rate of superficial vascular plexus formation (developmental angiogenesis) in retinas from P6 LysM WT and LysMCre-fur$^{(fl/fl)}$. In P6 neonatal mice, the diameters of retinal superficial vascular plexuses were similar and no differences in either the number of branching points or filopodia count were detected between LysMCre-fur$^{(fl/fl)}$ and LysM WT mice, indicating that furin expression by myeloid cells does not have a major influence on *in vivo* angiogenesis during neonatal development (Fig. 2A–E). This finding is in line with the above reported appearance of furin at the late stages of retinal vascular development (Fig. 1C).

2.4. Mice deficient for furin expression in myeloid cells show reduced hypoxic revascularization rate of the retina

The role of myeloid cell derived furin in hypoxia-driven neovascularization in the retina was explored next. First, we determined whether regression of vessels under hyperoxic conditions in the OIR model is comparable between LysMCre-fur$^{(fl/fl)}$ and LysM WT mice. After exposure to 75% oxygen between P7 and P12, retinas were evaluated at P12. Typical for this model (Smith et al., 1994; Uusitalo-Järvinen et al., 2007; Vähätupa et al., 2016b), large areas of the central vascular network were regressed with only a few major vessels remaining centrally in both LysM WT and LysMCre-fur$^{(fl/fl)}$ mice (Fig. 2F). Quantitative analysis of vaso-obliterated areas in retina confirmed that the retinal vasculature in LysMCre-fur$^{(fl/fl)}$ and LysM WT mice was similarly affected by hyperoxic exposure (Fig. 2G). Taken together, these data suggest that deletion of furin from myeloid cells has not a significant effect on vascular regression in OIR model.

On return to normoxia, the avascular central retina becomes hypoxic and stimulates rapid regrowth of vessels (Smith et al., 1994; Uusitalo-Järvinen et al., 2007). The rate of retinal revascularization in LysM WT and LysMCre-fur$^{(fl/fl)}$ retinas was determined by quantifying the avascular retinal area 5 days after the mice were returned to normoxia. There was a statistically significant difference in the avascular retinal area between the LysM WT and LysMCre-fur$^{(fl/fl)}$ mice at P17 showing that the rate of retinal revascularization is substantially (30%) reduced in mice where furin is depleted from myeloid cells (Fig. 2J). In addition to revascularization of the retina, the strong hypoxic stimulus from the center of the retina also drives abnormal misdirected sprouting of blood vessels towards the vitreous at the interface between the centrally obliterated and peripherally perfused retina (Smith et al., 1994; Uusitalo-Järvinen et al., 2007). This pathological, preretinal neovascularization reaches its maximum 5 days after return to normoxia (at P17). There was no statistically significant difference in the amount of preretinal neovascularization between LysM WT and

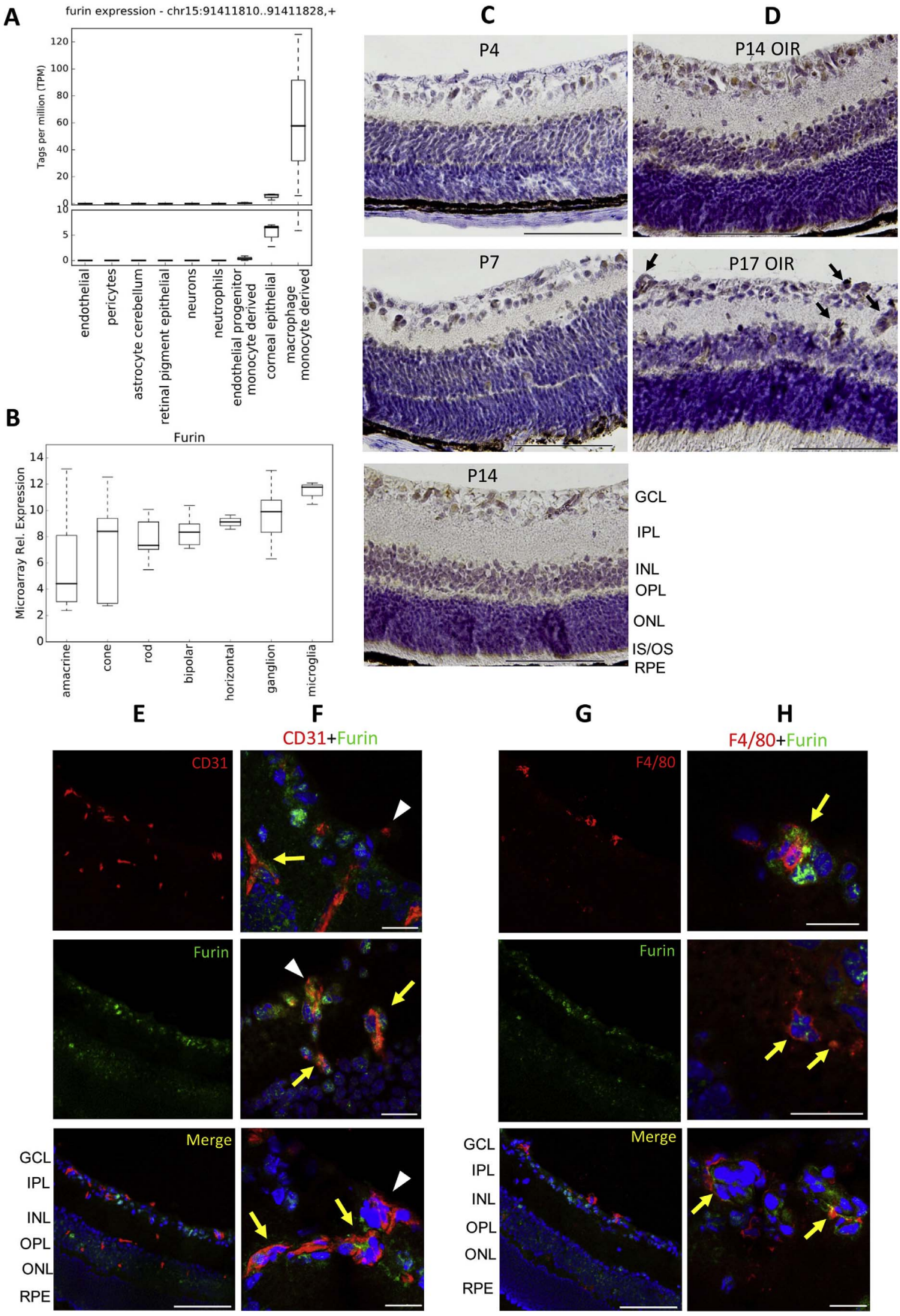

(caption on next page)

Fig. 1. Furin is expressed by the endothelial cells and macrophages in retina. Using expression data from the FANTOM 5 project, cDNA expression data was extracted for the primary furin CAGE for relevant cell types (A). Expression data for furin in different retinal cell types was extracted from previously performed microarray expression analysis (B). In panels A–B the cell types are sorted by increasing average expression from left to right. Furin expression from retina was determined during developmental angiogenesis at P4, P7 and P14 and in OIR model at P14 and P17 from the revascularized retinas by IHC and IF using furin specific antibody. Representative images of furin expression during development (C) and in the OIR model (D). Arrows are pointing furin specific staining at P17 OIR. Scale bars represents 100 μm. Representative confocal images showing CD31 positive endothelial cells (red) and furin (green) (E–F) and F4/80 positive macrophages (red) and furin (green) (G–H) in the retina of frozen sections after immunofluorescence staining. Panels E and G are showing stainings at 20× magnification and panels F and H at 63× magnification. Arrows are pointing the endothelial cells or macrophages that are expressing furin. Arrowheads are pointing neovascular tufts. GCL, ganglion cell layer; IPL, inner plexiform layer; INL, inner nuclear layer; OPL, outer plexiform layer; ONL, outer nuclear layer; IS/OS, photoreceptor inner/outer segments; RPE, retinal pigment epithelium. Scale bars represents 100 μm in E and G and 20 μm in F and H.

LysMCre-fur$^{(fl/fl)}$ retinas (Fig. 2K). The results indicate that myeloid cell expressed furin has a role in hypoxia-induced revascularization in retina, but does not influence the pathological preretinal neovascularization.

3. Discussion

The present study demonstrates that macrophages associated with retinal blood vessels express furin and the lack of furin in myeloid cells delays hypoxia-driven angiogenesis in retina. It has previously been shown that the endothelial specific deficiency of furin leads to embryonal death due to vascular defects (Roebroek et al., 1998), and the cultured endothelial cells lacking furin cannot grow (Kim et al., 2012). Our results confirm an important role for furin in angiogenesis as we show for the first time that furin deficiency in myeloid cells leads to impaired angiogenesis in hypoxia-induced retinal angiogenesis.

Previous studies have shown that resident macrophages, microglia, are needed for proper angiogenesis in retina during both developmental and hypoxia-induced angiogenesis (Checchin et al., 2006). In this study, we demonstrate that myeloid-cell specific deletion of proprotein convertase furin leads to the attenuation of angiogenesis and reduced vascularization rate in OIR model. Among furin's target proteins are several proangiogenic growth factors, including VEGF-C which is expressed in macrophages and has a role in controlling the branching of blood vessels in the retina (Siegfried et al., 2003a; Tammela et al., 2011). VEGF-A, in turn, does not require activating cleavage by furin. Interestingly, a myeloid-cell specific ablation of VEGF-A expression does not change the VEGF levels in the OIR and does not have any influence on angiogenesis in the OIR model (Liyanage et al., 2016). Although further studies concerning the role of furin in retinal angiogenesis are required, our results suggest that the expression of furin in macrophages may be related to activation of proangiogenic growth factors by furin in the retina. This is in line with previous studies showing simultaneous induction of VEGF-C and furin expression in different disease models (Khatib et al., 2010; Lopez de Cicco et al., 2004; Siegfried et al., 2003a).

A major function of furin is to control the bioavailability of anti-inflammatory TGF-β1 (Pesu et al., 2008). As a matter of fact, both furin and TGF-β are involved in the regulation of each other's activity; furin is needed for the activation of different TGF-β isoforms from inactive precursor molecules to active, mature forms (Pesu et al., 2008; Ventura et al., 2017). The active TGF-β2, in turn, induces furin expression (Ventura et al., 2017). Thus, together they generate a self-sustaining loop for high TGF-β activity (Ventura et al., 2017). TGF-β signaling is associated with neovascularization in many diseases, including neovascular ocular diseases (Amin et al., 1994; Bai et al., 2014; Wang et al., 2017). The expression of TGF-β is elevated in the OIR model, suggesting that TGF-β signaling contributes to retinal revascularization (Yingchuan et al., 2010). A previous study has shown that the TGF-β1 bioactivity is reduced in mice deficient in furin expression in myeloid cells (Cordova et al., 2016). Thus, another plausible explanation for the reduction of revascularization in the retina of LysMCre-fur$^{(fl/fl)}$ mice could be the reduced bioavailability of TGF-β due to lack of activating furin.

Although retinal revascularization rate and the formation of pathological preretinal tufts are inter-related in the OIR model, we identified a delayed revascularization rate in retina without a subsequent increase of pathological preretinal tuft formation in LysMCre-fur$^{(fl/fl)}$ mice in the OIR model. One explanation is that resident macrophages, microglia, persist in the retina in response to five-day long hyperoxia despite blood vessels disappearing completely from retina (Davies et al., 2006). Once the revascularization is initiated upon return to normoxia, i.e. induction of hypoxia in retina, resident microglial cells respond to hypoxia by secreting proangiogenic growth factors and direct the revascularization, but selectively only in retina, where they are located. This notion is supported by the facts that the microglia are mainly located in the avascular areas after the hyperoxia-period and the function of macrophage-derived VEGF-C is to convert the tip cells to stalk cells during retinal angiogenesis (Tammela et al., 2011). The lack of influence on preretinal pathological revascularization in the LysMCre-fur$^{(fl/fl)}$ mice is rather striking because we observed significantly larger avascular areas in LysMCre-fur$^{(fl/fl)}$ mice than in WT mice. This, in turn, should theoretically induce more pronounced compensatory preretinal pathological tuft formation, but we could not demonstrate that. An explanation why larger avascular retinal area does not translate into enhanced preretinal neovascularization, may be impaired proangiogenic growth factor activation in LysMCre-fur$^{(fl/fl)}$ mice.

Taken together our study demonstrates that the lack of furin in myeloid cells delays hypoxia-driven angiogenesis in retina and implicates furin expressed outside of the endothelial cells to the regulation of hypoxia-induced angiogenesis.

4. Methods

4.1. Mice

Monocyte/Macrophage-specific furin conditional knockout LysMCre-fur$^{(fl/fl)}$ was generated as described previously (Cordova et al., 2016). Briefly, mice bearing floxed *fur* alleles were backcrossed six times with C57BL/6 mice. LysMCre mice on C57BL/6 background were purchased from Taconic. LysMCre mice were bred with *fur*$^{(fl/fl)}$ animals to generate myeloid-specific furin knockout mice LysMCre-*fur*$^{(fl/fl)}$. Mice were housed under pathogen-free standard conditions, bred and the genotype was determined by PCR. Mice were fed with standard laboratory pellets and water *ad libitum*. All animal experiments were performed according to the ARVO statement for the use of animals in ophthalmic and vision research in accordance with protocols approved by the National Animal Ethics Committee of Finland.

4.2. Oxygen-induced retinopathy (OIR) model

The experiments on OIR model were carried out as described in detail previously (Smith et al., 1994; Stahl et al., 2010b; Uusitalo-Järvinen et al., 2007; Vähätupa et al., 2016b). Briefly, neonatal mice at P7 and their nursing mother were exposed to 75% oxygen for 5 days. At P12, the mice were returned to normal room air. Animals were euthanized at P12 to assess the degree of vascular regression and at P17 to determine the rate of retinal revascularization and preretinal neovascularization. As postnatal weight gain has been shown to affect outcome in the OIR model, the pups included in the study were weight-matched (Stahl et al., 2010a).

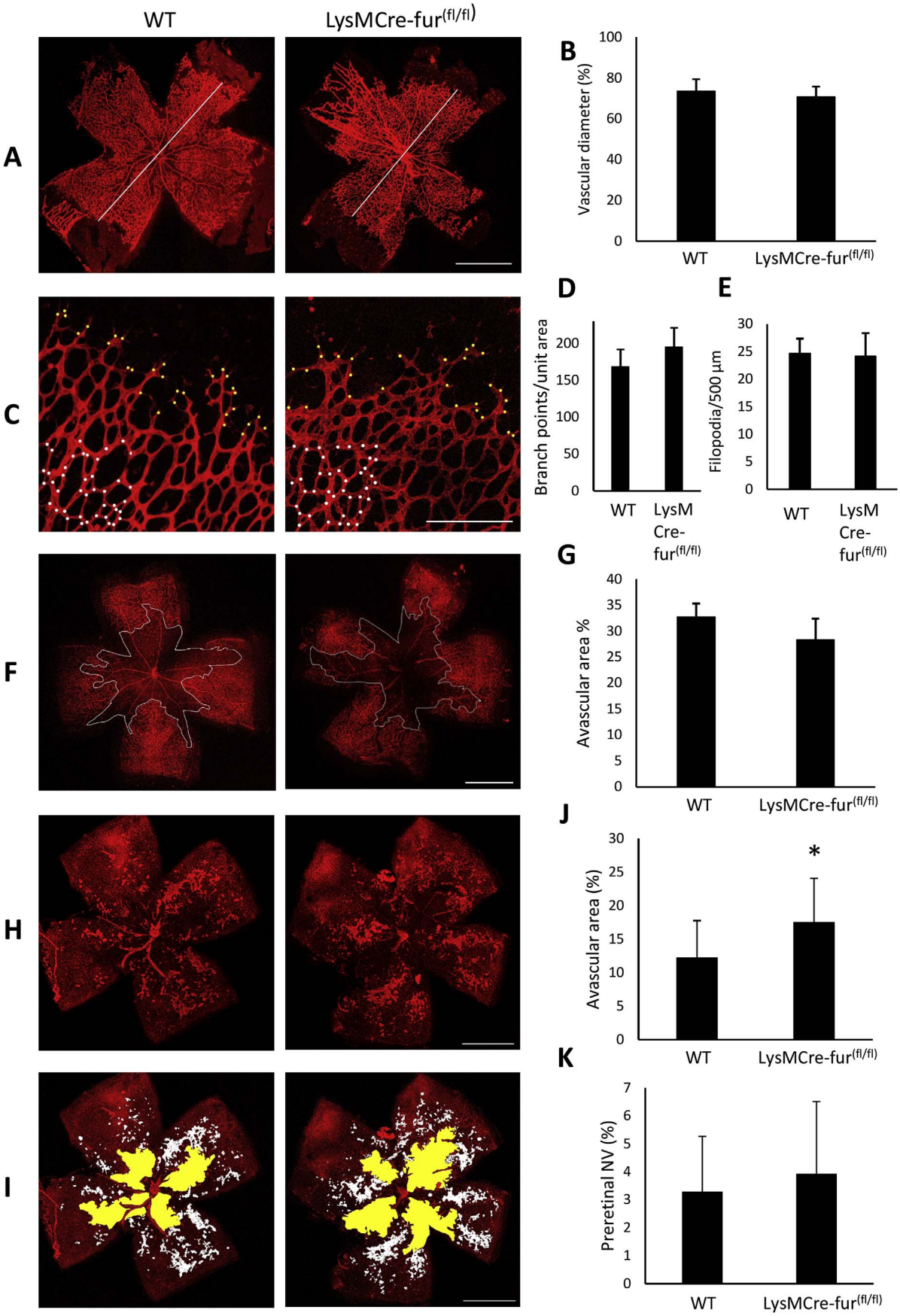

(caption on next page)

Fig. 2. Furin deficiency in myeloid cells inhibits revascularization rate in the retina during the OIR model. Eyes were harvested from healthy and LysMCre-fur($^{fl/fl}$) mice at P6 when the development of the superficial vascular plexus has occurred and in the OIR model at P12 and P17. Retinas were fixed with 4% PFA, flat mounted and stained with Alexa Fluor conjugated Isolectin IB_4. (A) The rate of early angiogenesis was quantified in retinal flat mounts by measuring the length of vasculature via the optic nerve. (B) There was no difference in the length of angiogenic vasculature of superficial vascular plexus between WT and LysMCre-fur($^{fl/fl}$) retinas at P6. (C) The number of branch points (white dots) in retinal vascular plexus and filopodia protrusions (yellow dots) from tip cells were counted from P6 retinas. The results are expressed as the number of branch points per unit area (D) and filopodia per 500 μm of vascular front (E). Both outcomes were similar between genotypes. WT n = 7 and KO n = 6. (F) Representative images of retinas right after the hyperoxic phase of OIR at P12. (G) Quantitative analysis of the avascular areas (inside the white line) shows that the vascular regression is similar in WT and LysMCre-fur($^{fl/fl}$) animals. (WT n = 4, KO n = 7 retinas.) (H) Representative OIR model retinas of WT and LysMCre-fur($^{fl/fl}$) mice at P17. (I) The avascular areas (yellow) and preretinal pathological neovascularization (tufts, white) were quantified. (J) Revascularization rate of retina is reduced by 30% ($p = 0.012$) in the LysMCre-fur($^{fl/fl}$) mice, while no differences were detected in the pathological revascularization, i.e. in the preretinal tufts (K). (WT n = 26 and KO n = 19 retinas.) Scale bar represents 1 mm in A, F, H and I and 200 μm in C. Error bars represent SDs.

4.3. FANTOM analysis of retinal cell types

The FANTOM project has performed expression analysis on 1839 samples from 573 primary cells, 152 tissues, and 250 cell lines in human. Specifically, the data comes from cap analysis gene expression (CAGE) sequencing of cDNA (FANTOM Consortium et al., 2014). Expression data was extracted for the primary furin CAGE for relevant cell types: endothelial cells, pericytes, astrocytes, retinal pigment epithelium cells, neurons, neutrophils, endothelial progenitor cells, corneal epithelial cells and monocyte derived macrophages.

4.4. Microarray analysis of retinal cell types

A microarray expression analysis of mouse genes in various retinal cell type groups was performed previously and is stored as accession E-GEOD-33089 on the ArrayExpress database (https://www.ebi.ac.uk/arrayexpress/experiments/E-GEOD-33089). From the data we extracted furin gene expression values for 155 samples across 7 cell type groups: amacrine, cone, rod, bipolar, horizontal, ganglion, and microglia (Siegert et al., 2012). Both FANTOM and microarray analyses were performed utilizing supercomputer resources provided by CSC–IT Center for Science of the Finnish Ministry of Education and Culture and the raw data was processed as previously described in detail elsewhere (Barker et al., 2017).

4.5. Immunohistochemistry (IHC) and isolectin GS-IB_4 staining

For immunohistochemistry, the eyes were fixed with 4% PFA and embedded in paraffin (for IHC), or freshly frozen in OCT embedding compound in liquid nitrogen cooled isopentane and later fixed with methanol (for immunofluorescence). The IHC stainings were carried out on 4–6 μm thick tissue sections using the following primary antibodies: rabbit anti-furin, (H-220), (Santa Cruz Biotechnology, Dallas, TX), rat anti-CD31 (BD Pharmingen, San Diego, CA) and rat anti-F4/80 (Life Technologies, Paisley, UK) followed by horseradish peroxidase (HRP) or fluorescein-conjugated secondary antibodies. Hematoxylin staining was used as a counterstain. IF samples were mounted with Vectashield mounting medium with DAPI (Vector Laboratories, Burlingame, CA) and images were taken with confocal microscope (Carl Zeiss LSM 700). As a negative control, each staining included sections stained without primary antibody.

4.6. Quantitative analysis of angiogenesis

For the analysis of retinal vasculature, eyes were enucleated, fixed with 4% PFA and retinas dissected. Flat mount retinas were blocked in 10% normal goat serum for 2 h, incubated overnight with Isolectin GS-IB_4 (1:200, Invitrogen, Carlsbad, CA) Retinas were imaged via confocal microscope (Carl Zeiss LSM 700) and the rate of angiogenesis was determined during development (P6) and in the OIR model as previously described (Connor et al., 2009; Stahl et al., 2010b). Briefly, retinas were imaged using confocal microscopy (Carl Zeiss LSM 700) with 10 × objective by focusing on the preretinal neovascular tufts and the underlying superficial vascular plexus. Areas of vascular obliteration and pathological neovascularization (neovascular tufts) were computed, in pixels, and divided by the total retinal area using Adobe Photoshop CS3. The rate of developmental angiogenesis at P6 was determined by measuring the diameter of vasculature via the optic nerve to the tips of the blood vessels. Analysis of vessel branching and number of filopodia sprouts were quantified as previously described (Lobov et al., 2007). Each point where three capillary segments met was counted as one junction. Branch points from the capillary plexus from two areas (370 μm × 550 μm) per retina were counted and results are shown by the average count per unit area. The number of filopodia protrusions from the tip cells were counted from the length of 500 μm of the sprouting vascular front (two measures per retina).

4.7. Statistical analysis

Student's t-test was conducted for normally distributed data and nonparametric Mann-Whitney *U* test (GraphPad Prism 6.01 and IBM SPSS statistics) for non-normally distributed data to test the statistical significance of the results. *P*-values less than 0.05 were considered statistically significant.

5. Statement of author contributions

M.V, T.J and H. U-J designed the research. M.V and H.B. performed the research. M.V, H.B, T.J and H. U-J analyzed the data. M.P, S.A and Z.M.C provided LysMCre-fur$^{(fl/fl)}$ mice for the study. M.V contributed the genotyped mice littermates. M.V, Z.M.C, H.B, T.J and H. U-J wrote the manuscript. M.V made the figures. All authors reviewed the paper.

Conflict of interest statement

The authors declare no conflict of interest.

Acknowledgements

We thank Marianne Karlsberg for excellent technical assistance. The work was supported by the Sigrid Juselius Foundation, the Academy of Finland, Päivikki and Sakari Sohlberg Foundation, Instrumentarium Research Foundation, Finnish Medical Foundation, Pirkanmaa Hospital District Research Foundation and the Finnish Cultural Foundation, Finnish Diabetic Research Foundation, Finnish Eye Foundation.

References

Abcouwer, S.F., 2012. Neural inflammation and the microglial response in diabetic retinopathy. J. Ocul. Biol. Dis. Infor 4, 25–33.
Amin, R., Puklin, J.E., Frank, R.N., 1994. Growth factor localization in choroidal neovascular membranes of age-related macular degeneration. Invest. Ophthalmol. Vis. Sci. 35, 3178–3188.
Bai, Y., Liang, S., Yu, W., Zhao, M., Huang, L., Zhao, M., Li, X., 2014. Semaphorin 3A blocks the formation of pathologic choroidal neovascularization induced by transforming growth factor β. Mol. Vis. 20, 1258–1270.
Barker, H., Aaltonen, M., Pan, P., Vähätupa, M., Kaipiainen, P., May, U., Prince, S., Uusitalo-Järvinen, H., Waheed, A., Pastorekova, S., Sly, W.S., Parkkila, S., Järvinen, T.A., 2017. Role of carbonic anhydrases in skin wound healing. Exp. Mol. Med. 49, e334.
Campochiaro, P.A., 2015. Molecular pathogenesis of retinal and choroidal vascular diseases. Prog. Retin. Eye Res. 49, 67–81.
Checchin, D., Sennlaub, F., Levavasseur, E., Leduc, M., Chemtob, S., 2006. Potential role of microglia in retinal blood vessel formation. Invest. Ophthalmol. Vis. Sci. 47,

3595–3602.
Connor, K.M., Krah, N.M., Dennison, R.J., Aderman, C.M., Chen, J., Guerin, K.I., Sapieha, P., Stahl, A., Willett, K.L., Smith, L.E., 2009. Quantification of oxygen-induced retinopathy in the mouse: a model of vessel loss, vessel regrowth and pathological angiogenesis. Nat. Protoc. 4, 1565–1573.
Cordova, Z.M., Gronholm, A., Kytola, V., Taverniti, V., Hamalainen, S., Aittomäki, S., Niininen, W., Junttila, I., Ylipaa, A., Nykter, M., Pesu, M., 2016. Myeloid cell expressed proprotein convertase FURIN attenuates inflammation. Oncotarget 23 7(34):54392–54404.
Cui, Y., Jean, F., Thomas, G., Christian, J.L., 1998. BMP-4 is proteolytically activated by furin and/or PC6 during vertebrate embryonic development. EMBO J. 17, 4735–4743.
Davies, M.H., Eubanks, J.P., Powers, M.R., 2006. Microglia and macrophages are increased in response to ischemia-induced retinopathy in the mouse retina. Mol. Vis. 12, 467–477.
Dubois, C.M., Blanchette, F., Laprise, M.H., Leduc, R., Grondin, F., Seidah, N.G., 2001. Evidence that furin is an authentic transforming growth factor-β1-converting enzyme. Am. J. Pathol. 158, 305–316.
FANTOM Consortium, the RIKEN PMI, CLST (DGT),Forrest, A.R., Kawaji, H., Rehli, M., Baillie, J.K., de Hoon, M.J., Haberle, V., Lassmann, T., Kulakovskiy, I.V., Lizio, M., Itoh, M., Andersson, R., Mungall, C.J., Meehan, T.F., Schmeier, S., Bertin, N., Jorgensen, M., Dimont, E., Arner, E., Schmidl, C., Schaefer, U., Medvedeva, Y.A., Plessy, C., Vitezic, M., Severin, J., Semple, C., Ishizu, Y., Young, R.S., Francescatto, M., Alam, I., Albanese, D., Altschuler, G.M., Arakawa, T., Archer, J.A., Arner, P., Babina, M., Rennie, S., Balwierz, P.J., Beckhouse, A.G., Pradhan-Bhatt, S., Blake, J.A., Blumenthal, A., Bodega, B., Bonetti, A., Briggs, J., Brombacher, F., Burroughs, A.M., Califano, A., Cannistraci, C.V., Carbajo, D., Chen, Y., Chierici, M., Ciani, Y., Clevers, H.C., Dalla, E., Davis, C.A., Detmar, M., Diehl, A.D., Dohi, T., Drablos, F., Edge, A.S., Edinger, M., Ekwall, K., Endoh, M., Enomoto, H., Fagiolini, M., Fairbairn, L., Fang, H., Farach-Carson, M.C., Faulkner, G.J., Favorov, A.V., Fisher, M.E., Frith, M.C., Fujita, R., Fukuda, S., Furlanello, C., Furino, M., Furusawa, J., Geijtenbeek, T.B., Gibson, A.P., Gingeras, T., Goldowitz, D., Gough, J., Guhl, S., Guler, R., Gustincich, S., Ha, T.J., Hamaguchi, M., Hara, M., Harbers, M., Harshbarger, J., Hasegawa, A., Hasegawa, Y., Hashimoto, T., Herlyn, M., Hitchens, K.J., Ho Sui, S.J., Hofmann, O.M., Hoof, I., Hori, F., Huminiecki, L., Iida, K., Ikawa, T., Jankovic, B.R., Jia, H., Joshi, A., Jurman, G., Kaczkowski, B., Kai, C., Kaida, K., Kaiho, A., Kajiyama, K., Kanamori-Katayama, M., Kasianov, A.S., Kasukawa, T., Katayama, S., Kato, S., Kawaguchi, S., Kawamoto, H., Kawamura, Y.I., Kawashima, T., Kempfle, J.S., Kenna, T.J., Kere, J., Khachigian, L.M., Kitamura, T., Klinken, S.P., Knox, A.J., Kojima, M., Kojima, S., Kondo, N., Koseki, H., Koyasu, S., Krampitz, S., Kubosaki, A., Kwon, A.T., Laros, J.F., Lee, W., Lennartsson, A., Li, K., Lilje, B., Lipovich, L., Mackay-Sim, A., Manabe, R., Mar, J.C., Marchand, B., Mathelier, A., Mejhert, N., Meynert, A., Mizuno, Y., de Lima Morais, D.A., Morikawa, H., Morimoto, M., Moro, K., Motakis, E., Motohashi, H., Mummery, C.L., Murata, M., Nagao-Sato, S., Nakachi, Y., Nakahara, F., Nakamura, T., Nakamura, Y., Nakazato, K., van Nimwegen, E., Ninomiya, N., Nishiyori, H., Noma, S., Noma, S., Noazaki, T., Ogishima, S., Ohkura, N., Ohimiya, H., Ohno, H., Ohshima, M., Okada-Hatakeyama, M., Okazaki, Y., Orlando, V., Ovchinnikov, D.A., Pain, A., Passier, R., Patrikakis, M., Persson, H., Piazza, S., Prendergast, J.G., Rackham, O.J., Ramilowski, J.A., Rashid, M., Ravasi, T., Rizzu, P., Roncador, M., Roy, S., Rye, M.B., Saijyo, E., Sajantila, A., Saka, A., Sakaguchi, S., Sakai, M., Sato, H., Savvi, S., Saxena, A., Schneider, C., Schultes, E.A., Schulze-Tanzil, G.G., Schwegmann, A., Sengstag, T., Sheng, G., Shimoji, H., Shimoni, Y., Shin, J.W., Simon, C., Sugiyama, D., Sugiyama, T., Suzuki, M., Suzuki, N., Swoboda, R.K., t Hoen, P.A., Tagami, M., Takahashi, N., Takai, J., Tanaka, H., Tatsukawa, H., Tatum, Z., Thompson, M., Toyodo, H., Toyoda, T., Valen, E., van de Wetering, M., van den Berg, L.M., Verado, R., Vijayan, D., Vorontsov, I.E., Wasserman, W.W., Watanabe, S., Wells, C.A., Winteringham, L.N., Wolvetang, E., Wood, E.J., Yamaguchi, Y., Yamamoto, M., Yoneda, M., Yonekura, Y., Yoshida, S., Zabierowski, S.E., Zhang, P.G., Zhao, X., Zucchelli, S., Summers, K.M., Suzuki, H., Daub, C.O., Kawai, J., Heutink, P., Hide, W., Freeman, T.C., Lenhard, B., Bajic, V.B., Taylor, M.S., Makeev, V.J., Sandelin, A., Hume, D.A., Carninci, P., Hayashizaki, Y., 2014. A promoter-level mammalian expression atlas. Nature 507, 462–470.
Fong, D.S., Aiello, L., Gardner, T.W., King, G.L., Blankenship, G., Cavallerano, J.D., Ferris 3rd, F.L., Klein, R., American Diabetes Association, 2004. Retinopathy in diabetes. Diabetes Care 27 (Suppl. 1), S84–S87.
Gao, X., Wang, Y.S., Li, X.Q., Hou, H.Y., Su, J.B., Yao, L.B., Zhang, J., 2016. Macrophages promote vasculogenesis of retinal neovascularization in an oxygen-induced retinopathy model in mice. Cell Tissue Res. 364, 599–610.
Jonas, J.B., Mones, J., Glacet-Bernard, A., Coscas, G., 2017. Retinal vein occlusions. Dev. Ophthalmol. 58, 139–167.
Kanda, A., Noda, K., Saito, W., Ishida, S., 2012. (Pro)renin receptor is associated with angiogenic activity in proliferative diabetic retinopathy. Diabetologia 55, 3104–3113.
Kataoka, K., Nishiguchi, K.M., Kaneko, H., van Rooijen, N., Kachi, S., Terasaki, H., 2011. The roles of vitreal macrophages and circulating leukocytes in retinal neovascularization. Invest. Ophthalmol. Vis. Sci. 52, 1431–1438.
Khatib, A.M., Lahlil, R., Scamuffa, N., Akimenko, M.A., Ernest, S., Lomri, A., Lalou, C., Seidah, N.G., Villoutreix, B.O., Calvo, F., Siegfried, G., 2010. Zebrafish ProVEGF-C expression, proteolytic processing and inhibitory effect of unprocessed ProVEGF-C during fin regeneration. PLoS One 5, e11438.
Kim, W., Essalmani, R., Szumska, D., Creemers, J.W., Roebroek, A.J., D'Orleans-Juste, P., Bhattacharya, S., Seidah, N.G., Prat, A., 2012. Loss of endothelial furin leads to cardiac malformation and early postnatal death. Mol. Cell. Biol. 32, 3382–3391.
Liyanage, S.E., Fantin, A., Villacampa, P., Lange, C.A., Denti, L., Cristante, E., Smith, A.J., Ali, R.R., Luhmann, U.F., Bainbridge, J.W., Ruhrberg, C., 2016. Myeloid-derived vascular endothelial growth factor and hypoxia-inducible factor are dispensable for ocular neovascularization–brief report. Arterioscler. Thromb. Vasc. Biol. 36, 19–24.
Lobov, I.B., Renard, R.A., Papadopoulos, N., Gale, N.W., Thurston, G., Yancopoulos, G.D., Wiegand, S.J., 2007. Delta-like ligand 4 (Dll4) is induced by VEGF as a negative regulator of angiogenic sprouting. Proc. Natl. Acad. Sci. U. S. A. 104, 3219–3224.
Lopez de Cicco, R., Watson, J.C., Bassi, D.E., Litwin, S., Klein-Szanto, A.J., 2004. Simultaneous expression of furin and vascular endothelial growth factor in human oral tongue squamous cell carcinoma progression. Clin. Cancer Res. 10, 4480–4488.
Ma, J., Evrard, S., Badiola, I., Siegfried, G., Khatib, A.M., 2017. Regulation of the proprotein convertases expression and activity during regenerative angiogenesis: role of hypoxia-inducible factor (HIF). Eur. J. Cell Biol. 96, 457–468.
McColl, B.K., Paavonen, K., Karnezis, T., Harris, N.C., Davydova, N., Rothacker, J., Nice, E.C., Harder, K.W., Roufail, S., Hibbs, M.L., Rogers, P.A., Alitalo, K., Stacker, S.A., Achen, M.G., 2007. Proprotein convertases promote processing of VEGF-D, a critical step for binding the angiogenic receptor VEGFR-2. FASEB J. 21, 1088–1098.
McMahon, S., Grondin, F., McDonald, P.P., Richard, D.E., Dubois, C.M., 2005. Hypoxia-enhanced expression of the proprotein convertase furin is mediated by hypoxia-inducible factor-1: impact on the bioactivation of proproteins. J. Biol. Chem. 280, 6561–6569.
Mitamura, Y., Harada, C., Harada, T., 2005. Role of cytokines and trophic factors in the pathogenesis of diabetic retinopathy. Curr. Diabetes Rev. 1, 73–81.
Oksanen, A., Aittomäki, S., Jankovic, D., Ortutay, Z., Pulkkinen, K., Hamalainen, S., Rokka, A., Corthals, G.L., Watford, W.T., Junttila, I., O'Shea, J.J., Pesu, M., 2014. Proprotein convertase FURIN constrain Th2 differentiation and is critical for host resistance against Toxoplasma gondii. J. Immunol. 193, 5470–5479.
Pesu, M., Watford, W.T., Wei, L., Xu, L., Fuss, I., Strober, W., Andersson, J., Shevach, E.M., Quezado, M., Bouladoux, N., Roebroek, A., Belkaid, Y., Creemers, J., O'Shea, J.J., 2008. T-cell-expressed proprotein convertase furin is essential for maintenance of peripheral immune tolerance. Nature 455, 246–250.
Reynolds, J.D., 2014. Insights in ROP. Am. Orthopt. J. 64, 43–53.
Roebroek, A.J., Umans, L., Pauli, I.G., Robertson, E.J., van Leuven, F., Van de Ven, W.J., Constam, D.B., 1998. Failure of ventral closure and axial rotation in embryos lacking the proprotein convertase Furin. Development 125, 4863–4876.
Scamuffa, N., Calvo, F., Chretien, M., Seidah, N.G., Khatib, A.M., 2006. Proprotein convertases: lessons from knockouts. FASEB J. 20, 1954–1963.
Siegert, S., Cabuy, E., Scherf, B.G., Kohler, H., Panda, S., Le, Y.Z., Fehling, H.J., Gaidatzis, D., Stadler, M.B., Roska, B., 2012. Transcriptional code and disease map for adult retinal cell types. Nat. Neurosci. 15 487–495, S1-2.
Siegfried, G., Basak, A., Cromlish, J.A., Benjannet, S., Marcinkiewicz, J., Chretien, M., Seidah, N.G., Khatib, A.M., 2003a. The secretory proprotein convertases furin, PC5, and PC7 activate VEGF-C to induce tumorigenesis. J. Clin. Invest. 111, 1723–1732.
Siegfried, G., Khatib, A.M., Benjannet, S., Chretien, M., Seidah, N.G., 2003b. The proteolytic processing of pro-platelet-derived growth factor-A at RRKR(86) by members of the proprotein convertase family is functionally correlated to platelet-derived growth factor-A-induced functions and tumorigenicity. Cancer Res. 63, 1458–1463.
Siegfried, G., Basak, A., Prichett-Pejic, W., Scamuffa, N., Ma, L., Benjannet, S., Veinot, J.P., Calvo, F., Seidah, N., Khatib, A.M., 2005. Regulation of the stepwise proteolytic cleavage and secretion of PDGF-B by the proprotein convertases. Oncogene 24, 6925–6935.
Silvestri, L., Pagani, A., Camaschella, C., 2008. Furin-mediated release of soluble hemojuvelin: a new link between hypoxia and iron homeostasis. Blood 111, 924–931.
Smith, L.E., Wesolowski, E., McLellan, A., Kostyk, S.K., D'Amato, R., Sullivan, R., D'Amore, P.A., 1994. Oxygen-induced retinopathy in the mouse. Invest. Ophthalmol. Vis. Sci. 35, 101–111.
Stahl, A., Chen, J., Sapieha, P., Seaward, M.R., Krah, N.M., Dennison, R.J., Favazza, T., Bucher, F., Lofqvist, C., Ong, H., Hellstrom, A., Chemtob, S., Akula, J.D., Smith, L.E., 2010a. Postnatal weight gain modifies severity and functional outcome of oxygen-induced proliferative retinopathy. Am. J. Pathol. 177, 2715–2723.
Stahl, A., Connor, K.M., Sapieha, P., Chen, J., Dennison, R.J., Krah, N.M., Seaward, M.R., Willett, K.L., Aderman, C.M., Guerin, K.I., Hua, J., Lofqvist, C., Hellstrom, A., Smith, L.E., 2010b. The mouse retina as an angiogenesis model. Invest. Ophthalmol. Vis. Sci. 51, 2813–2826.
Tammela, T., Zarkada, G., Nurmi, H., Jakobsson, L., Heinolainen, K., Tvorogov, D., Zheng, W., Franco, C.A., Murtomaki, A., Aranda, E., Miura, N., Yla-Herttuala, S., Fruttiger, M., Makinen, T., Eichmann, A., Pollard, J.W., Gerhardt, H., Alitalo, K., 2011. VEGFR-3 controls tip to stalk conversion at vessel fusion sites by reinforcing Notch signalling. Nat. Cell Biol. 13, 1202–1213.
Tsutsumi, C., Sonoda, K.H., Egashira, K., Qiao, H., Hisatomi, T., Nakao, S., Ishibashi, M., Charo, I.F., Sakamoto, T., Murata, T., Ishibashi, T., 2003. The critical role of ocular-infiltrating macrophages in the development of choroidal neovascularization. J. Leukoc. Biol. 74, 25–32.
Turpeinen, H., Ortutay, Z., Pesu, M., 2013. Genetics of the first seven proprotein convertase enzymes in health and disease. Curr. Genomics 14, 453–467.
Uusitalo-Järvinen, H., Kurokawa, T., Mueller, B.M., Andrade-Gordon, P., Friedlander, M., Ruf, W., 2007. Role of protease activated receptor 1 and 2 signaling in hypoxia-induced angiogenesis. Arterioscler. Thromb. Vasc. Biol. 27, 1456–1462.
Vähätupa, M., Aittomäki, S., Martinez Cordova, Z., May, U., Prince, S., Uusitalo-Järvinen, H., Järvinen, T.A., Pesu, M., 2016a. T-cell-expressed proprotein convertase FURIN inhibits DMBA/TPA-induced skin cancer development. Oncoimmunology 5, e1245266.
Vähätupa, M., Prince, S., Vataja, S., Mertimo, T., Kataja, M., Kinnunen, K., Marjomaki, V., Uusitalo, H., Komatsu, M., Järvinen, T.A., Uusitalo-Järvinen, H., 2016b. Lack of r-ras leads to increased vascular permeability in ischemic retinopathy. Invest. Ophthalmol. Vis. Sci. 57, 4898–4909.
Ventura, E., Weller, M., Burghardt, I., 2017. Cutting edge: ERK1 mediates the autocrine positive feedback loop of TGFβ and furin in glioma-initiating cells. J. Immunol. 198, 4569–4574.

Wang, X., Ma, W., Han, S., Meng, Z., Zhao, L., Yin, Y., Wang, Y., Li, J., 2017. TGFβ participates choroid neovascularization through Smad2/3-VEGF/TNF-α signaling in mice with Laser-induced wet age-related macular degeneration. Sci. Rep. 7 9672–017-10124-4.

Yingchuan, F., Chuntao, L., Hui, C., Jianbin, H., 2010. Increased expression of TGF-β1 and Smad 4 on oxygen-induced retinopathy in neonatal mice. Adv. Exp. Med. Biol. 664, 71–77.

Zhou, Y., Yoshida, S., Nakao, S., Yoshimura, T., Kobayashi, Y., Nakama, T., Kubo, Y., Miyawaki, K., Yamaguchi, M., Ishikawa, K., Oshima, Y., Akashi, K., Ishibashi, T., 2015. M2 macrophages enhance pathological neovascularization in the mouse model of oxygen-induced retinopathy. Invest. Ophthalmol. Vis. Sci. 56, 4767–4777.